

Zero-Space Cost Fault Tolerance for Transformer-based Language Models on ReRAM

Bingbing Li
bingbing.li@uconn.edu
University of Connecticut
USA

Geng Yuan
geng.yuan@uga.edu
University of Georgia
USA

Zigeng Wang
zigeng.wang@uconn.edu
University of Connecticut
USA

Shaoyi Huang
shaoyi.huang@uconn.edu
University of Connecticut
USA

Hongwu Peng
hongwu.peng@uconn.edu
University of Connecticut
USA

Payman Behnam
payman.behnam@gatech.edu
Georgia Institute of Technology
USA

Wujie Wen
wwen2@ncsu.edu
North Carolina State University
USA

Hang Liu
hang.liu@rutgers.edu
Rutgers
USA

Caiwen Ding
caiwen.ding@uconn.edu
University of Connecticut
USA

ABSTRACT

Resistive Random Access Memory (ReRAM) has emerged as a promising platform for deep neural networks (DNNs) due to its support for parallel in-situ matrix-vector multiplication. However, hardware failures, such as stuck-at-fault defects, can result in significant prediction errors during model inference. While additional crossbars can be used to address these failures, they come with storage overhead and are not efficient in terms of space, energy, and cost. In this paper, we propose a fault protection mechanism that incurs zero space cost. Our approach includes: 1) differentiable structure pruning of rows and columns to reduce model redundancy, 2) weight duplication and voting for robust output, and 3) embedding duplicated most significant bits (MSBs) into the model weight. We evaluate our method on nine tasks of the GLUE benchmark with the BERT model, and experimental results prove its effectiveness.

KEYWORDS

ReRAM, fault tolerance, compression, Transformer, BERT

1 INTRODUCTION

Resistive Random Access Memory (ReRAM), a non-volatile memory based on programmable resistance, provides both data storage and in-situ dot product calculations to accelerate DNN inference. Several ReRAM-based neural accelerators, such as PRIME [1] and ISAAC [2], have been proposed for energy-efficient applications.

However, due to the immaturity of fabrication technology, ReRAM-based systems can suffer from possible failures. Permanent faults, known as hard faults, cause the resistance states of ReRAM cells to be fixed at high resistance (stuck-at-0 fault) or low resistance (stuck-at-1 fault), due to fabrication defects [3]. In the case of deep neural network inference, the impact of hardware failure is amplified as errors in the front layers accumulate and propagate layer by layer during forward propagation. The situation becomes worse for the application of large scale natural language processing (NLP) models, such as BERT [4], GPT [5], etc. Before applying these models on ReRAM platforms, the weight parameters are quantized [6] and binarized into bit matrices, consisting of the most significant bits (MSBs) and least significant bits (LSBs). Among these bit matrices,

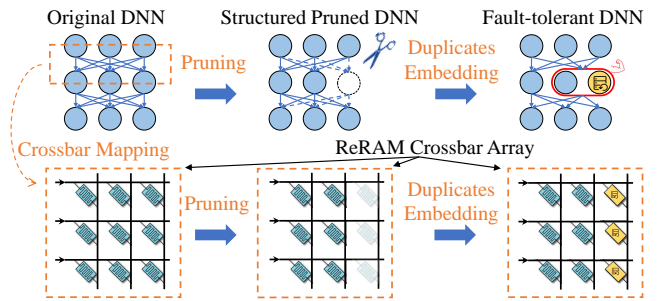


Figure 1: Zero-space Cost Fault Tolerance on ReRAM.

the MSBs have the most significant impact on model performance. Stuck-at-1 failures, which occur more than 5 times as frequently as stuck-at-0 failures, can increase parameter values by 10 or even 100 times, leading to significant degradation in model performance. In this paper, we focus on MSB failure tolerance.

Different methods are proposed to mitigate the effects of hardware failures [3, 7–11]. Liu [7] proposed an on-device training method by generating a dedicated network that can tolerate faults in the memristor chip distribution. Chen [3] proposed a “write-verify” scheme that involves conducting online tests and repairs regularly to address faults. In order to achieve a balance between robustness and accuracy on ReRAM, Wang [11] proposed a fault-tolerant training scheme to enhance resilience to stuck-at-fault defects. However, these approaches introduce storage overhead and require additional ReRAM modules and auxiliary ADC/DAC circuits. This raises the question: Can we improve the robustness of the model on ReRAM without incurring storage overhead? Fortunately, the answer is yes. By leveraging model pruning and compression techniques, we can obtain a sparse model structure and save a significant number of ReRAM modules and ADC/DAC circuits.

DNN networks are commonly acknowledged to have a significant level of redundancy. To address this issue and ensure model accuracy, pruning methods such as deep compression [12] and heuristic pruning [13] as well as quantization methods like fixed-point [14] and binarization [15] have been proposed and utilized. Structured pruning methods, such as efficient pruning [16] and FTrans [17], have also been proposed to improve the efficiency of

hardware and have shown significant acceleration gains on actual hardware. However, these methods rely on manual parameter selection and fine-tuning based on human experience. Additionally, they require customized debugging for different DNN models, such as adopting different sparsity expectations for different layers [18]. In order to reduce the need for manual intervention, Xiao [19] proposed automatic pruning, which automatically finds the optimal sparse model structure by incorporating trainable auxiliary parameters.

Our motivation for this research is twofold: 1) given that some parameters are both crucial and prone to errors, why not create backups for these parameters to improve the overall model’s robustness? 2) since DNNs contain a significant amount of redundancy, can’t these redundancies be leveraged to compensate for the additional hardware introduced by the backups?

In this paper, we propose a fault tolerance strategy that does not introduce additional parameter space. We present an automatic structured (specifically, row and column) pruning method to reduce the parameter space and use these pruned parameter space to store important backup parameters. Furthermore, we introduce a weight voting strategy to enhance the robustness of the entire network. Our contributions in this paper can be summarized as follows:

- We propose a novel structured differentiable pruning method, the row and column differentiable pruning, to achieve row and column sparsity in the model automatically. We use gate parameters to determine which rows or columns to retain and update both the gate and weight parameters to achieve a better balance between model accuracy and sparsity.
- Based on the observation that most of the parameter values are smaller than the half of the maximal value of the corresponding layer, we introduce a bit-flipping voting strategy to leverage the duplicated parameters to recover the original output and improve the final model’s performance.
- We propose an MSB embedding method to eliminate the storage overhead introduced by the duplicated parameters. Specifically, we adopt an in-place redundant duplicates storage strategy by embedding these duplicated MSBs into the model weights during weight-crossbar mapping on ReRAM.

2 BACKGROUND AND LIMITATION

2.1 ReRAM-based systems: Advantage and Limitations

Deep Neural Networks (DNNs) have become dominant in the field of artificial intelligence due to their high accuracy and scalability. As DNN models have grown in size, they present great challenges for conventional hardware due to the increasing computational cost and memory storage requirements. However, the weights and computing units are separated in the conventional Von Neumann architectures, which results in significant data movements [20].

Resistive Random Access Memory (ReRAM), compared to conventional accelerators, has shown superior performance in terms of inference speed boosting, extremely low energy consumption, and in-situ computation. This is attributed to the fact that ReRAM crossbars can naturally reduce data movements and computation costs, thus accelerating DNNs.

Despite the high hardware efficiency enjoyed by ReRAM-based Computation Systems (RCS), ReRAM circuits are still prone to hardware faults due to immature fabrication technology. These faults can be categorized into hard faults and soft faults. Soft faults include Read-One-Disturb (R1D) and Read-Zero-Disturb (R0D), while the most common types of hard faults are Stuck-At-Faults (SAF), which include Stuck-At-Zero (SA0) and Stuck-At-One (SA1) [21]. In the case of soft faults, an ReRAM cell can still function since its resistance can change. However, for hard faults, the previous solution is not applicable anymore due to the unchangeable resistance. Consequently, weights cannot be programmed into the faulty cell. This leads to a significant drop in accuracy since the matrix stored in a crossbar is incomplete. The inference accuracy is sensitive to the number of defective memristors [22, 23].

2.2 Pruning for efficient ReRAM utilization

In the pruning strategy, magnitude-based pruning methods such as ADMM [18] and Reweighted L1 [24] can reduce redundant model parameters by assigning the expected sparsity for each layer. However, this approach often suffers from sub-optimal results, as the pruning performance relies solely on the researchers’ experience. To address this limitation, various efficient one-shot automatic pruning algorithms have been proposed, in which the pruned model structure and weights are jointly learned through back-propagation. Another solution for sparse model structure searching is reinforcement learning. However, this method requires extensive training time due to the large search space and relies heavily on the researcher’s experience to achieve stable training performance.

Differentiable pruning, on the other hand, assigns auxiliary parameters to determine the weight retention and updates these parameters using back-propagation. This approach can achieve a high compression ratio while maintaining model accuracy. Unlike earlier methods, differentiable pruning does not rely on layer-wise sparsity design and can determine the layer sparsity automatically. Straight-through estimators (STEs) [19, 25] are introduced in pruning to learn discrete sparse network structures. These estimators assign overridden coarse gradients to binarization functions. Differentiable neural network architecture search with Gumbel Softmax [26] and the use of Gumbel Softmax in attention head pruning [27] for transformer models have also been proposed. However, neither of these algorithms has implemented differentiable pruning schemes for structured pruning to enhance hardware computation efficiency.

3 FAULT-TOLERATED RERAM

To improve the hardware efficiency and robustness of SAF, we propose a fault-tolerated ReRAM implementation method that involves: 1) leveraging differentiable structured pruning to remove redundant weights while preserving model accuracy, 2) introducing weight voting strategy by leveraging the duplicated bits for fault tolerance of the Most Significant Bits (MSBs) to maintain model accuracy, 3) introducing an in-place duplicates storage strategy by embedding these duplicated bits into the model weights during weight-crossbar mapping.

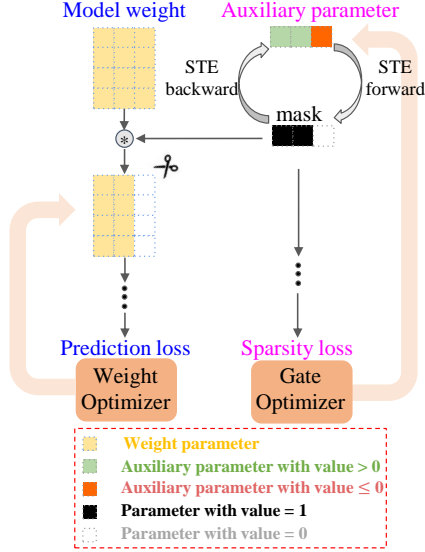


Figure 2: Differentiable structured (e.g. column) pruning framework.

3.1 Stage 1: Differentiable structured pruning

Structured pruning is performed to reduce model redundancy by dropping entire weights in different rows or columns of weight matrix, thus achieving a row- or column-sparse model architecture.

For an N -layer DNN model, the weight parameters of the k -th layer are denoted as W_k . The pruning problem can be formulated based on L_0 regularization:

$$\operatorname{argmin}_W f(X, \{W_k\}_{k=1}^N) + \mu \sum_{k=1}^N \|\{W_k\}_{k=1}^N\|_{l_0}, \quad (1)$$

where $f(*)$ denotes the accuracy loss function representing the model prediction loss, X represents the model input, and μ represents the penalty factor of model sparsity.

To overcome the optimization problem of L_0 regularization and prune the weights in a back-propagation manner, we introduce an indicator function, $H(*)$, to represent the pruning status of the model weights. For structured pruning, we formulate the row pruning function, H_{row} , and column pruning function, H_{col} , as follows:

$$H_{row}(W_k; M_k) = \operatorname{Concat}_i(M_k \otimes W[i, :], \dim = 0) \quad (2)$$

$$H_{col}(W_k; M_k) = \operatorname{Concat}_j(M_k^T \otimes W[:, j], \dim = 1) \quad (3)$$

$$M_k[i] = \begin{cases} 0, & \text{if } W[i, :] \text{ or } W[:, i] \text{ is pruned;} \\ 1, & \text{otherwise.} \end{cases} \quad (4)$$

where $\operatorname{Concat}(*)$ represents the concatenating function to concatenate different rows or columns according to \dim selection, M_i is a column vector and represents the binary mask for the structure (row or column), $W[i, :]$ represents the i -th row of the weight matrix and $W[:, j]$ represents the j -th column, \otimes represents the Kronecker product [28].

Then the structured pruning problem can be reformulated as the following optimization problem:

$$\operatorname{argmin}_{W, M} f(X, \{H(W_k; M_k)\}_{k=1}^N) + \mu \sum_{k=1}^N \|\{M_k\}_{k=1}^N\|_{l_1} \quad (5)$$

To make it differentiable in Eq.5, we employ learnable discrete functions called straight through estimators (STEs) [15, 19] g to describe the mask M and thus M can be formulated as:

$$M_k[i] = g(W'_k[i]) = \begin{cases} 0, & \text{if } W'_k[i] \leq 0 \\ 1, & \text{if } W'_k[i] > 0. \end{cases} \quad (6)$$

where W'_k is the auxiliary parameter to control the open and close of the binary masking gate M_k , and M_k is represented as a step function g with a continuous auxiliary parameter W'_k .

Finally, we formulate the structured pruning problem as:

$$\operatorname{argmin}_{W, W'} \mathcal{L}_t = \operatorname{argmin}_{W, W'} \left[f\{X, H(W_k; g(W'_k))\}_{k=1}^N + \mu \sum_{k=1}^N \|g(W'_k)\|_{l_1} \right] \quad (7)$$

where \mathcal{L}_t is the total loss during structured pruning.

The problem described in Eq. 7 is a mixed integer programming problem. We design two optimizers: weight optimizer to update retained model weight using normal back-propagation and gate optimizer to update auxiliary parameter as shown in Fig 2. The binary gates are non-differentiable and we introduce coarse gradients [15] to calculate the gradient of the binarization function. We use Softplus STE in [19] and the auxiliary parameter W' can be updated as:

$$W' \leftarrow W' - l_{rg} * \frac{\partial \mathcal{L}_t}{\partial W'} \quad (9)$$

$$\frac{\mathcal{L}_t}{\partial W'} = \frac{\partial \mathcal{L}_t}{\partial M} * \frac{\partial M}{\partial W'} = \frac{\partial \mathcal{L}_t}{\partial M} * \operatorname{Softplus}(W') \quad (10)$$

where l_{rg} is the learning rate of the gate optimizer to update W' .

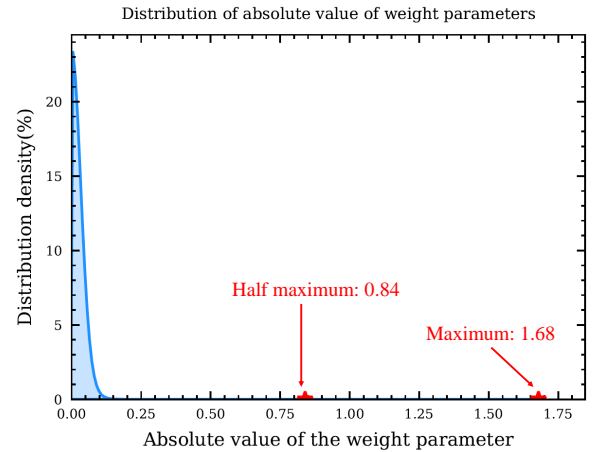


Figure 3: Weight distribution of the 1st layer weight matrix of BERT model: most values of the parameters are much smaller than the half of the weight maximum.

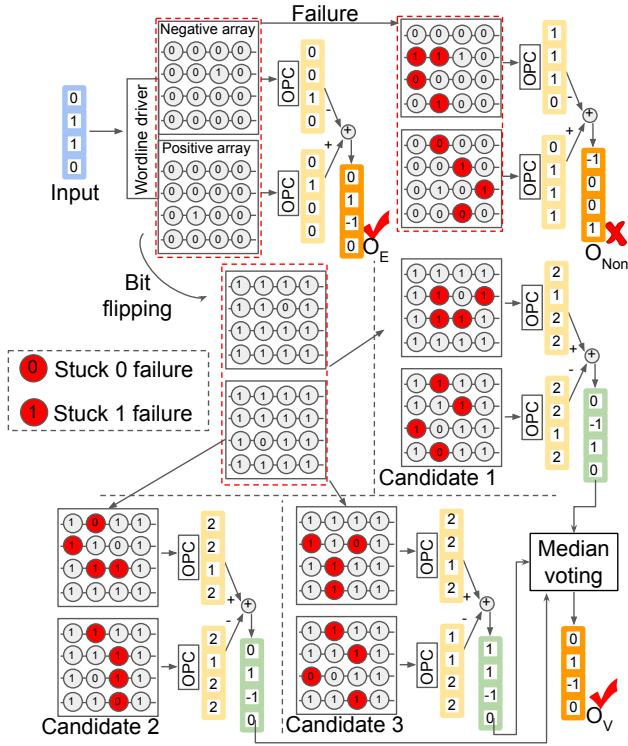


Figure 4: Duplication and output voting on ReRAM crossbars (O_E is the expected output, O_{Non} is the output without voting, O_V is the output after voting, OPC module is the Output Peripheral Component).

3.2 Stage 2: Fault tolerance

The occurrence of hard faults can lead to significant degradation in model performance. In the case of single-bit implementation of ReRAM-based systems, the normal fault ratio can exceed 0.05%. Furthermore, the occurrence of a Stuck-At-Faults (SAF) on the most significant bits (MSBs) can result in a weight value change of up to $10\times$ or even $100\times$, which is disastrous during model inference. Figure 3 shows the weight distribution of the first encoder layer in BERT, where the maximum absolute value is 1.68, while more than 99% absolute weight values are smaller than half of the maximum. This illustrates the high risk of significant value change in model weights with MSB SA1 fault since more than 99% of MSBs values are zero.

To improve fault tolerance, we first duplicate MSBs while mapping model weights to ReRAM crossbars. During inference on ReRAM, we use these duplicates as candidates to vote for the final circuit output. Additionally, to leverage the weight parameter distribution finding, we design a bit-flipping voting strategy by mapping flipped bits into the ReRAM platform and changing the sign of the obtained intermediate results. This is due to two reasons: 1) since more than 99% model parameter values are smaller than the half of the maximum, more than 99% MSBs are zero, which is severely sensitive to SAF; 2) the frequency of SA1 failure is much larger than SA0 [29].

Algorithm 1: Model inference with MSB fault tolerance for each layer

Input: weight matrix W , layer input X , number of candidates T
Output: model layer output O
 Do n -bit quantization and binarization of W to obtain $B = [MSB, LSB_{n-1}, \dots, LSB_1]$;
 Duplicate and bit-flip MSB T times to obtain MSB_1, \dots, MSB_T ;
foreach duplicate MSB_k **do**
 Add SA0 and SA1 failure noise into MSB_k to simulate SAF;
 Calculate the candidate output of MSB_k as O_{MSB_k} by using OPCs and summing;
end
 Do median voting using $[O_{MSB_1}, \dots, O_{MSB_T}]$ to derive the final MSB array output O_{MSB} ;
 Calculate the output of $[LSB_{n-1}, \dots, LSB_1]$ as $[O_{LSB_{n-1}}, \dots, O_{LSB_1}]$;
 Use $[O_{MSB}, O_{LSB_{n-1}}, \dots, O_{LSB_1}]$ to derive the final output O .

3.2.1 Quantization and binarization. In order to facilitate hardware implementations, we employ n -bit equal-distance quantization, resulting in a total of $V = 2^{n-1}$ quantization levels. Specifically, for each layer weight W_k , we obtain the quantized weight matrix, W_q , by quantizing the weights into a set of quantization values $\{-\frac{V}{2}q_i, \dots, -q_i, q_i, \dots, \frac{V}{2}q_i\}$, where $q_i = \max(\text{abs}(W_k)) / (2^{n-1})$.

The quantized weights are then binarized as follows:

$$W_q = \text{Sign} * (MSB * 2^{n-1} + LSB_{n-1} * 2^{n-2} + \dots + LSB_1 * 1) \quad (11)$$

where **Sign** is the sign matrix of W , **MSB** represents the most significant bit (MSB) matrix of W_q , and **LSB** represents the less significant bit (LSB) matrix of W_q . During ReRAM crossbar mapping, the **Sign** matrix is not directly mapped to the crossbars. Instead, we use a negative ReRAM array and a positive ReRAM array to represent the **Sign** matrix.

3.2.2 MSB duplication and result voting. After quantization and binarization of the model, we obtain binary weights consisting of MSBs and LSBs. Since MSBs has the most significant impact on model performance, we duplicate the MSB matrices and design the output voting strategy to enhance the resilience to SAF defects on ReRAM.

Before voting, we use a 0-1 flipped bit matrix for model weight and crossbar mapping. To store the weight sign, negative and positive arrays are used to store the negative and positive values of the model weight. Instead of directly mapping the weight bit value to the crossbars, we invert the bit value between 0 and 1, and map the inverted bit value into the negative and positive crossbar arrays.

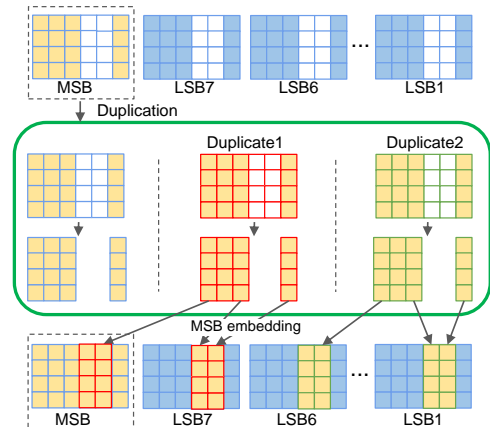


Figure 5: MSB embedding to eliminate storage overhead.

During inference, we calculate the candidate outputs by changing the sign of the output of the Output Peripheral Components (OPCs) before summing, and use the median value of the three candidate results as the final layer output. The entire process is illustrated in Figure 4 and Algorithm 1. In our test, we manually add SA0 and SA1 faults to simulate the ReRAM SAF by giving different hardware failure rate.

3.3 Stage 3: Embedding MSB candidates for weight-crossbar mapping

To address the storage overhead introduced by MSBs duplication, we adopt an in-place redundant duplicates storage strategy by embedding these backup MSBs into the model weights during mapping.

The process of inserting additional MSB columns into the positions of zero columns after structured pruning is depicted in Figure 5 and Algorithm 2. In the case of 8-bit quantization, if the sparsity (percentage of pruned columns) exceeds 30%, there is no additional storage overhead introduced. Figure 6 showcases the weight-crossbar mapping in real ReRAM modules, where the duplicated MSBs columns are mapped to the positions corresponding to zero model weights. As described in Section 4.2, the derived sparse models have more than 30% sparsity on all nine datasets, demonstrating the eliminated storage overhead.

4 EVALUATION

4.1 Experiment settings

Our baseline model is the BERT-base-uncased model from HuggingFace [30]. To evaluate the performance of the pruned model, we use the GLUE benchmark, which consists of 9 tasks covering different categories of NLP tasks with different degrees of difficulty and dataset scales. We report accuracy scores for SST-2, QNLI, RTE, and WNLI; Matthews Correlation Coefficient (MCC) for CoLA; F1 scores for QQP and MRPC; and Spearman correlations for STS-B. For BERT, we use the official BERT_{BASE} uncased model as our pre-trained model. This model has 12 layers ($L = 12$; hidden size $H = 768$; self-attention heads $A = 12$), with total number of parameters of 110 million. We use the same fine-tuning hyperparameters as described in [4].

4.2 Results of differentiable structured pruning

We compared the performance of our pruned models with the baseline models (unpruned models) and summarized the results in

Algorithm 2: ReRAM crossbar mapping with zero space cost for one layer

Input: sparse MSB₁, sparse LSBs, additional MSBs (MSB₂, MSB₃, ..., MSB_K), column pruning index **Index**
Output: Mapped crossbar arrays with embedded MSBs
 Set additional bit matrix **A** as an empty list;
foreach each MSB_k ($k = 2, \dots, K$) **do**
 foreach each column of MSB_k **do**
 if column index is not in **Index** **then**
 append column into **A**
 end
 end
end
 Distribute **A** into zero columns of MSB₁ and LSBs.

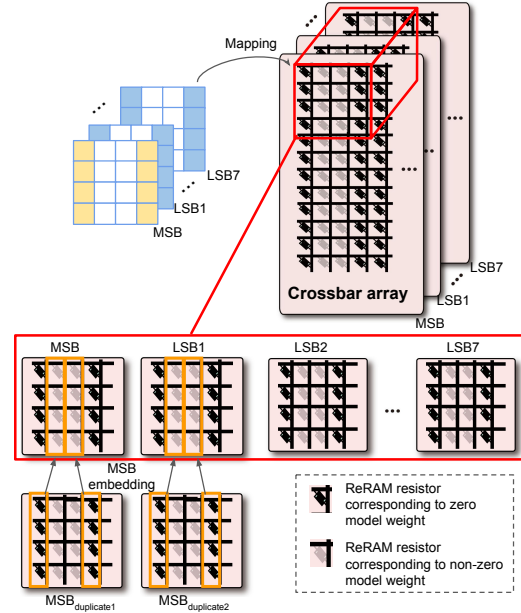


Figure 6: Duplicated MSBs embedding

Table 1. As mentioned in Section 3.2.2, we consider sparsities larger than 30% to meet the MSB embedding requirements. Across all nine tasks, we achieved more than 30% sparsity with either no or less than 1% drop in accuracy. Surprisingly, our pruned models even showed accuracy improvements on the QNLI, CoLA, and MRPC datasets, which could be attributed to the reduction of redundant weights that led to decreased overfitting. Moreover, our models successfully met the requirement of eliminating the introduced storage overhead for all tasks in the GLUE benchmark.

4.3 Distribution of weight parameters

To gain a better understanding of the weight parameter distribution and further contribute to the mapping and voting improvement, we analyzed the weight distribution of word embedding layer and all 12 encoder layers of the BERT model. Table 2 presents the distribution of the absolute values of the model parameters in different layers. The maximum value represents the highest value within the entire layer and we define the *large parameters* as the parameters with the values larger than the half of the maximum of the corresponding weight matrix. We counted the number of large parameters and observed that more than 99% of the weight parameters were smaller than half of the maximal value of the weight matrix. Consequently, more than 99% of the MSB elements are zeros. This proves the effectiveness of the bit-flipping strategy during weight-crossbar mapping.

4.4 MSB candidates voting

As described in Section 3.2.2, we simulate ReRAM failures (SA0 and SA1 failures) by introducing 0 or 1 noise. We set the overall failure ratio to follow the widely-used SA0 and SA1 ratio of 1.75:9.04 [3, 29]. Figure 7 displays the model accuracy with and without candidate voting when different percentages of ReRAM failures are introduced. The results demonstrate the significant improvement in accuracy preserving with voting. With a 0.05% failure rate, our voting method

Table 1: Differentiable structured pruning among the nine GLUE benchmark tasks.

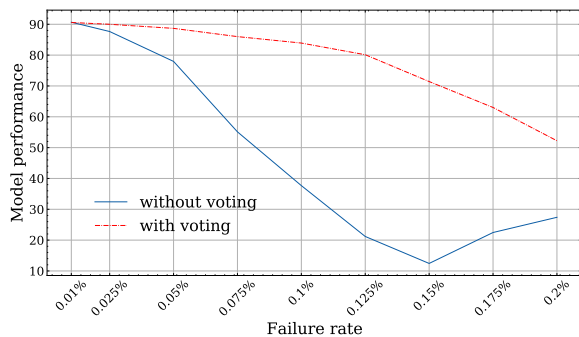
Models	MNLI	QQP	QNLI	SST-2	CoLA	STS-B	MRPC	RTE	WNLI
BERT _{BASE} [4]	84.6	91.2	90.5	93.5	52.1	85.8	88.9	66.4	-
BERT _{BASE} (ours)	83.9	91.4	91.1	92.7	53.4	85.8	89.8	66.4	56.3
BERT _{BASE} prune (ours)	83.19	90.86	90.72	92.75	54.72	85.73	89.74	66.79	56.34
Sparsity	36.2%	30.03%	31.53	40.13%	31.60%	30.42%	31.35%	42.22%	45.64%

Table 2: Distribution of the absolute values of the model weight paramters (WB: Word Embedding layer; E: Encoder layer)

	WB	E1	E2	E3	E4	E5	E6	E7	E8	E9	E10	E11	E12
#param(million)	23.44	2.36	2.36	2.36	2.36	2.36	2.36	2.36	2.36	2.36	2.36	2.36	2.36
param maximum	0.95	1.68	2.15	3.33	6.64	6.82	6.02	4.81	3.56	3.13	3.08	6.37	2.15
#(large param)	7	6	18	2	3	1	1	1	2	4	14	2	5

Table 3: Model performance with different failure rates with and without failure tolerance with BERT on MRPC dataset.

Method		Failure rate								
		0.01%	0.025%	0.05%	0.075%	0.1%	0.125%	0.15%	0.175%	0.2%
Without voting	Accuracy Mean	90.68	87.65	77.96	55.11	37.68	21.18	12.44	22.47	27.40
	Accuracy Variance	0.36	0.97	14.35	169.49	286.78	227.09	178.24	231.09	269.88
With voting (ours)	Accuracy Mean	90.58	90.26	88.68	86	83.91	80.13	71.43	63.02	52.23
	Accuracy Variance	0.20	0.50	1.20	2.33	4.85	10.23	50.74	93.22	155.73

**Figure 7: Model performance with different failure rates with and without output voting on MRPC.**

achieves an accuracy improvement of nearly 10% over the baseline model without voting at the same failure rate. Moreover, our method can tolerate 2.5 times the failure rate compared to the baseline, while maintaining a drop in accuracy below 10%.

5 CONCLUSION

In this paper, we propose a fault tolerance strategy without introducing additional parameter space on ReRAM. Differentiable structured pruning method is proposed to automatically reduce model redundancy and a fault-tolerant model inference method based on bit-flipping, most significant bits (MSBs) duplication, and result voting to enhance the capability to handle Stuck-at-fault (SAF) defects on ReRAM. Additionally, we embed the MSBs duplicates into the pruned zero parameter space to eliminate the storage overhead. Experimental results show that our pruning method can remove enough parameter space to eliminate the storage space overhead (larger than 30%) of the introduced duplicates, while the model performance is maintained with either no or less than 1% accuracy drop on all nine GLUE datasets. For the SAF defects, the proposed method can tolerate 2.5 times the failure rate with the same model accuracy as the baseline, which proves the effectiveness to enhance the resilience to ReRAM SAF defects.

REFERENCES

- [1] Ping Chi, Shuangchen Li, Cong Xu, Tao Zhang, Jishen Zhao, Yongpan Liu, Yu Wang, and Yuan Xie. Prime: A novel processing-in-memory architecture for neural network computation in ream-based main memory. *ACM SIGARCH Computer Architecture News*, 44(3):27–39, 2016.
- [2] Ali Shafiee, Anirban Nag, Naveen Muralimanohar, Rajeev Balasubramonian, John Paul Strachan, Miao Hu, R Stanley Williams, and Vivek Srikumar. Isaac: A convolutional neural network accelerator with in-situ analog arithmetic in crossbars. In *Proceedings of the 43rd International Symposium on Computer Architecture*, pages 14–26. IEEE Press, 2016.
- [3] Ching-Yi Chen, Hsiu-Chuan Shih, Cheng-Wen Wu, Chih-He Lin, Pi-Feng Chiu, Shyh-Shyuan Sheu, and Frederick T Chen. Ram defect modeling and failure analysis based on march test and a novel squeeze-search scheme. *IEEE Transactions on Computers*, 64(1):180–190, 2014.
- [4] Jacob Devlin, Ming-Wei Chang, Kenton Lee, and Kristina Toutanova. Bert: Pre-training of deep bidirectional transformers for language understanding. *arXiv preprint arXiv:1810.04805*, 2018.
- [5] Alec Radford, Jeffrey Wu, Rewon Child, David Luan, Dario Amodei, and Ilya Sutskever. Language models are unsupervised multitask learners.
- [6] Eunhyeok Park, Junwhan Ahn, and Sungjoo Yoo. Weighted-entropy-based quantization for deep neural networks. In *Proceedings of the IEEE Conference on Computer Vision and Pattern Recognition*, pages 5456–5464, 2017.
- [7] Beiye Liu, Hai Li, Yiran Chen, Xin Li, Qing Wu, and Tingwen Huang. Vortex: Variation-aware training for memristor x-bar. In *Proceedings of the 52nd Annual Design Automation Conference*, pages 1–6, 2015.
- [8] Zheyu Yan, Xiaobo Sharon Hu, and Yiyu Shi. Computing-in-memory neural network accelerators for safety-critical systems: Can small device variations be disastrous? In *2022 IEEE/ACM International Conference On Computer Aided Design (ICCAD)*, pages 1–9. IEEE, 2022.
- [9] Zheyu Yan, Sharon X Hu, and Yiyu Shi. Swim: Selectivewrite-verify for computing-in-memory neural accelerators. In *Proceedings of the IEEE/ACM Design Automation Conference*, 2022.
- [10] Zheyu Yan, Yifan Qin, Wujie Wen, Xiaobo Sharon Hu, and Yiyu Shi. Improving realistic worst-case performance of nvcim dnn accelerators through training with right-censored gaussian noise. In *2023 IEEE/ACM International Conference on Computer Aided Design (ICCAD)*, pages 1–9. IEEE, 2023.
- [11] Sijue Wang, Geng Yuan, Xiaolong Ma, Yanyu Li, Xue Lin, and Bhavya Kaikhura. Fault-tolerant deep neural networks for processing-in-memory based autonomous edge systems. In *2022 Design, Automation & Test in Europe Conference & Exhibition (DATE)*, pages 424–429. IEEE, 2022.
- [12] Song Han, Huizi Mao, and William J Dally. Deep compression: Compressing deep neural networks with pruning, trained quantization and huffman coding. *International Conference on Learning Representations (ICLR)*, 2016.
- [13] Xiaoliang Dai, Hongxu Yin, and Niraj Jha. Nest: A neural network synthesis tool based on a grow-and-prune paradigm. *IEEE Transactions on Computers*, 2019.
- [14] Darryl Lin, Sachin Talathi, and Sreekanth Annapureddy. Fixed point quantization of deep convolutional networks. In *International Conference on Machine Learning*, pages 2849–2858, 2016.

- [15] Itay Hubara, Matthieu Courbariaux, Daniel Soudry, Ran El-Yaniv, and Yoshua Bengio. Binarized neural networks. *Advances in neural information processing systems*, 29, 2016.
- [16] Bingbing Li, Zhenglun Kong, Tianyun Zhang, Ji Li, Zhengang Li, Hang Liu, and Caiwen Ding. Efficient transformer-based large scale language representations using hardware-friendly block structured pruning. In *Findings of the Association for Computational Linguistics: EMNLP 2020*, pages 3187–3199, 2020.
- [17] Bingbing Li, Santosh Pandey, Haowen Fang, Yanjun Lyv, Ji Li, Jieyang Chen, Mimi Xie, Lipeng Wan, Hang Liu, and Caiwen Ding. Ftrans: energy-efficient acceleration of transformers using fpga. In *Proceedings of the ACM/IEEE International Symposium on Low Power Electronics and Design*, pages 175–180, 2020.
- [18] Tianyun Zhang, Shaokai Ye, Kaiqi Zhang, Jian Tang, Wujie Wen, Makan Fardad, and Yanzhi Wang. A systematic dnn weight pruning framework using alternating direction method of multipliers. In *Proceedings of the European Conference on Computer Vision (ECCV)*, pages 184–199, 2018.
- [19] Xia Xiao, Zigeng Wang, and Sanguthevar Rajasekaran. Autoprune: Automatic network pruning by regularizing auxiliary parameters. *Advances in neural information processing systems*, 32, 2019.
- [20] Geng Yuan, Payman Behnam, Zhengang Li, Ali Shafiee, Sheng Lin, Xiaolong Ma, Hang Liu, Xuehai Qian, Mahdi Nazm Bojnordi, Yanzhi Wang, and Caiwen Ding. Forms: Fine-grained polarized rram-based in-situ computation for mixed-signal dnn accelerator. In *2021 ACM/IEEE 48th Annual International Symposium on Computer Architecture (ISCA)*, pages 265–278, 2021.
- [21] Ching-Yi Chen, Hsiu-Chuan Shih, Cheng-Wen Wu, Chih-He Lin, Pi-Feng Chiu, Shyh-Shyuan Sheu, and Frederick T. Chen. Rram defect modeling and failure analysis based on march test and a novel squeeze-search scheme. *IEEE Transactions on Computers*, 64(1):180–190, 2015.
- [22] Baogang Zhang, Necati Uysal, Deliang Fan, and Rickard Ewetz. Handling stuck-at-faults in memristor crossbar arrays using matrix transformations. In *Proceedings of the 24th Asia and South Pacific Design Automation Conference, ASPDAC '19*, page 438–443, New York, NY, USA, 2019. Association for Computing Machinery.
- [23] Haoqiang Guo, Lu Peng, Jian Zhang, Qing Chen, and Travis D LeCompte. Att: A fault-tolerant rram accelerator for attention-based neural networks. In *2020 IEEE 38th International Conference on Computer Design (ICCD)*, pages 213–221, 2020.
- [24] Tianyun Zhang, Xiaolong Ma, Zheng Zhan, Shanglin Zhou, Caiwen Ding, Makan Fardad, and Yanzhi Wang. A unified dnn weight pruning framework using reweighted optimization methods. In *2021 58th ACM/IEEE Design Automation Conference (DAC)*, pages 493–498. IEEE, 2021.
- [25] Suraj Srinivas, Akshayvarun Subramanya, and R Venkatesh Babu. Training sparse neural networks. In *Proceedings of the IEEE Conference on Computer Vision and Pattern Recognition*, pages 138–145, 2017.
- [26] Hanxiao Liu, Karen Simonyan, and Yiming Yang. Darts: Differentiable architecture search. In *International Conference on Learning Representations*, 2018.
- [27] Elena Voita, David Talbot, Fedor Moiseev, Rico Sennrich, and Ivan Titov. Analyzing multi-head self-attention: Specialized heads do the heavy lifting, the rest can be pruned. In *Proceedings of the 57th Annual Meeting of the Association for Computational Linguistics*, pages 5797–5808, 2019.
- [28] Horn Roger and R Johnson Charles. Topics in matrix analysis, 1994.
- [29] Beckmann Karsten et al. Nanoscale hafnium oxide rram devices exhibit pulse dependent behavior and multi-level resistance capability. *Mrs Advances*, 1(49):3355–3360, 2016.
- [30] Wolf Thomas et al. Transformers: State-of-the-art natural language processing. In *Proceedings of the 2020 conference on empirical methods in natural language processing: system demonstrations*, pages 38–45, 2020.